Original Research Article

Lithofacies Analysis of Multistorey Braidplain Sandstone, Lokoja-Bassange Formation, Benin Flank of Anambra Basin, Nigeria

ABSTRACT

A braidplain sandstone body in the Cretaceous Lokoja-Bassange Formation was studied for the purpose of classifying its constituent sediment facies, developing a conceptual sedimentological model that reflects its alluvial architecture, and assessing the implications of this architecture for reservoir development. The NE-SW trending sandstone is approximately 1.2 km long, 55 m wide and, at least, 15 m thick.

Four sedimentary logs, produced at selected points across the sandstone body, were combined with its sedimentary attributes to construct a conceptual sedimentological model that captures its geometrical framework. The morphology of the channel sandstone is classified into three groups based on decreasing magnitude: (1) cross-bedded, tabular morphology with sheet geometry, extending to maximum length of 1200 m and maximum thickness of 15 m, (2) multistorey channel morphology with laterally stacked geometry, extending to 90 m in length and 8 m in thickness, and (3) single channel morphology with lenticular geometry, extending over lateral and vertical distances of 2-5 m and 1.7 m, respectively. Amalgamation of beds is common, enabling thick laterally extensive channel-fill sequence to develop. The sequence consists of pebbly sandstone and medium to very coarse sandstone with claystone clasts that are randomly distributed.

The sedimentological model suggests that the Campanian braidplain sandstone has a complex history of bar migration that produced laterally-stacked multistorey channel sandstone. This architecture will facilitate effective pressure communication across producing reservoir intervals. Lack of organized stratification and discontinuous shales may turn these reservoirs into a single hydraulic unit with effective lateral displacement of fluids to production wells. Such laterally connected channel sandstone, however, requires a trapping mechanism for hydrocarbon to accumulate and impermeable floodplain mudstone to preserve it. Laterally extensive floodplain mudstone, on the other hand, poses a major risk to vertical flow because of its potential for flow segregation across net pay intervals.

Keywords: Braidplain, channel morphology, sedimentological model, alluvial architecture, pressure communication

1. INTRODUCTION

Braidplain deposits are products of low-sinuosity braided river systems. These deposits can occur on a continental scale with very large systems over 40 km wide and 1200 m thick [1]. They have excellent quality and are known to be very productive hydrocarbon reservoirs and aquifers [2, 3, 4, 5]. Prolific hydrocarbon reservoirs that are known to be deposited in braidplain depositional setting are found in Prudhoe Bay field [6] and Endicott field in Alaska [7]; Sirte field [8], Sarir field [2], and Messla field [9] in Libya; Cooper and Eromanga Basins fields in Australia [10, 11]; Recôncavo Basin fields in Brazil [12, 13]; Alwyn North field in

United Kingdom [14]; Statfjord field in the Norwegian North Sea [15]; Marib Al Jawf Basin fields in Yemen [16, 17]; and more.

Within the braidplain, braided river flows across and between the diverse range of bars, thus splitting in the upstream of bars and joining in the downstream [18]. Avulsion is a common character of these rivers, and it displaces flow into a new channel position, abandoning its original course and flowing in a different part of the low-lying area. As a result of this complex behaviour, sandbodies with similar textural characteristics may display different geometries and facies types with complex internal architecture [1, 4, 5]. These complexities may have a profound effect on sedimentary attributes of constituent facies and flow communication between pay intervals in braidplain successions.

OBJECTIVES OF STUDY: (HIGHLIGHT IT IN CLEAR POINTS)

This outcrop-based study aims to classify facies types in the braidplain sandstone of Cretaceous Lokoja-Bassange Formation in the Benin flank of Anambra Basin. It presents a conceptual sedimentological model that captures geometrical framework of the sandstone body, and thus, provides valuable insights into its alluvial architecture and hydrocarbon exploration potential.

2. MATERIAL AND METHODS

2.1 Outcrop Description and Geological Setting

The outcrop selected for this study is situated between Latitudes N 07°07'14" and N 07°08'38", and Longitudes E 06°13'00" and E 06°14'20". It is exposed as a road cut along Igarra-Auchi road in Edo State, southern Nigeria (Figure 1). It is well exposed and covers an estimated area of 169650 m^2. Maximum exposed length of the sandstone is 1200 m along northeast to southwest and its maximum exposed width in the north-south direction is 55 m. The outcrop represents the exposed part of the Cretaceous Lokoja-Bassange Formation in the Benin Flank of Anambra Basin. This basin, which is located in Southern Benue Trough, is a NE-SW trending intracratonic rift basin [19, 20] that borders Bida Basin and northern Nigerian Massif in the north and the Tertiary Niger Delta Basin in the south. To the west, the basin borders the West African Massif, and to the east, the middle Benue Trough and Abakaliki Anticlinorium (Figure 2).

The break-up of the Gondwana Supercontinent during late Jurassic times [21] led to the tectonic evolution of the Anambra Basin. Following the break-up, convection currents dominated the asthenosphere and led to the separation of African and South American plates. Consequently, a failed arm of an RRR triple junction was developed in the early Cretaceous [22]. The irregular subsidence of the eastern half of the southern Benue Trough caused profound magmatism, folding and uplifting that led to flexural inversion of the Abakaliki area and developed into Abakaliki Anticlinorium [23], and subsequently caused the exposure and erosion of the Coniacian, Turonian and Albian Formations. These depressions

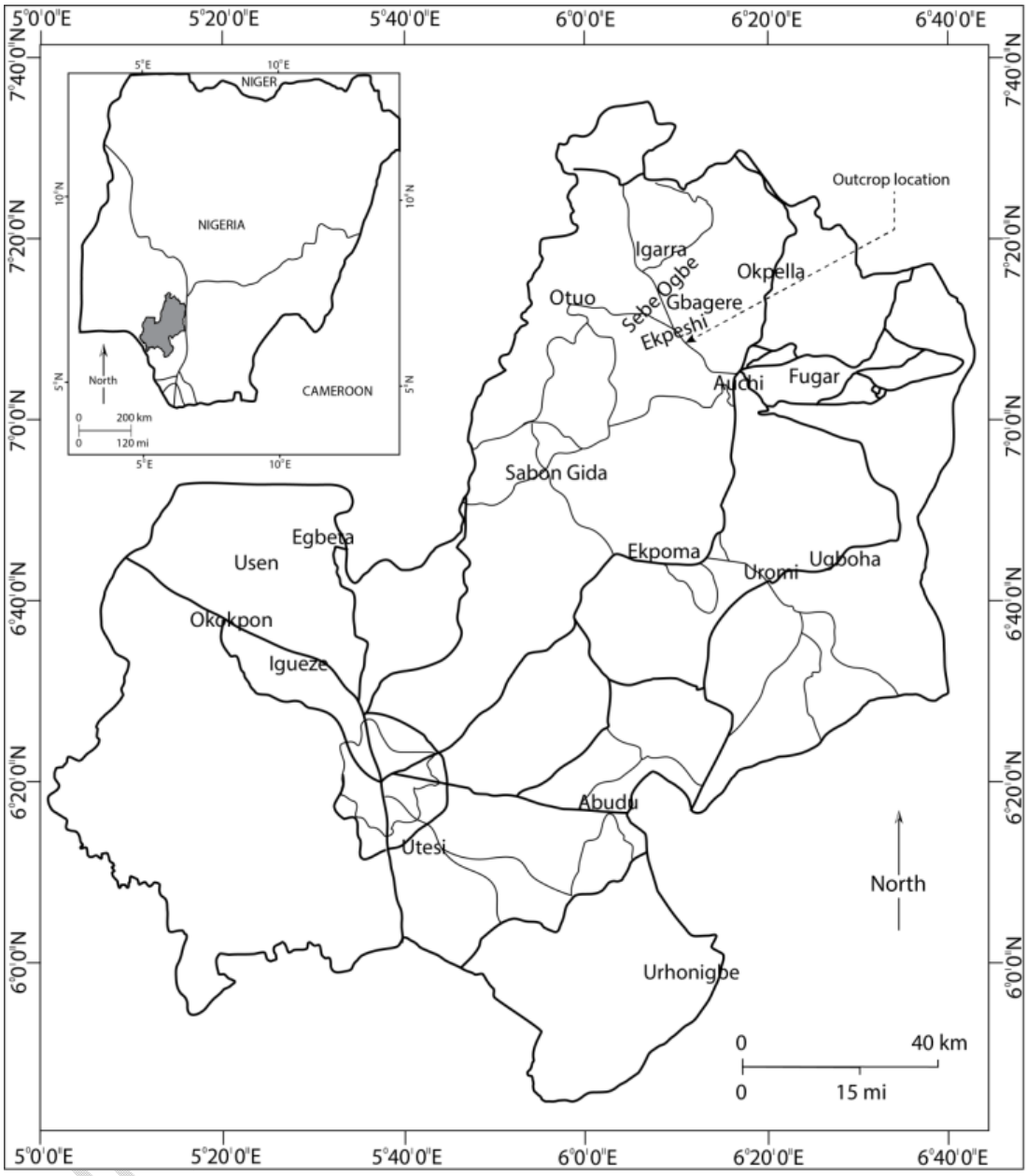

Figure 1. Map of Edo State, Nigeria (reproduced from Google map). Lokoja-Bassange Formation outcrops at Ekpeshi Town (see dotted line north of the map) along Igarra-Auchi Road, Edo State. Inset: Map of Nigeria indicating location of Edo State.

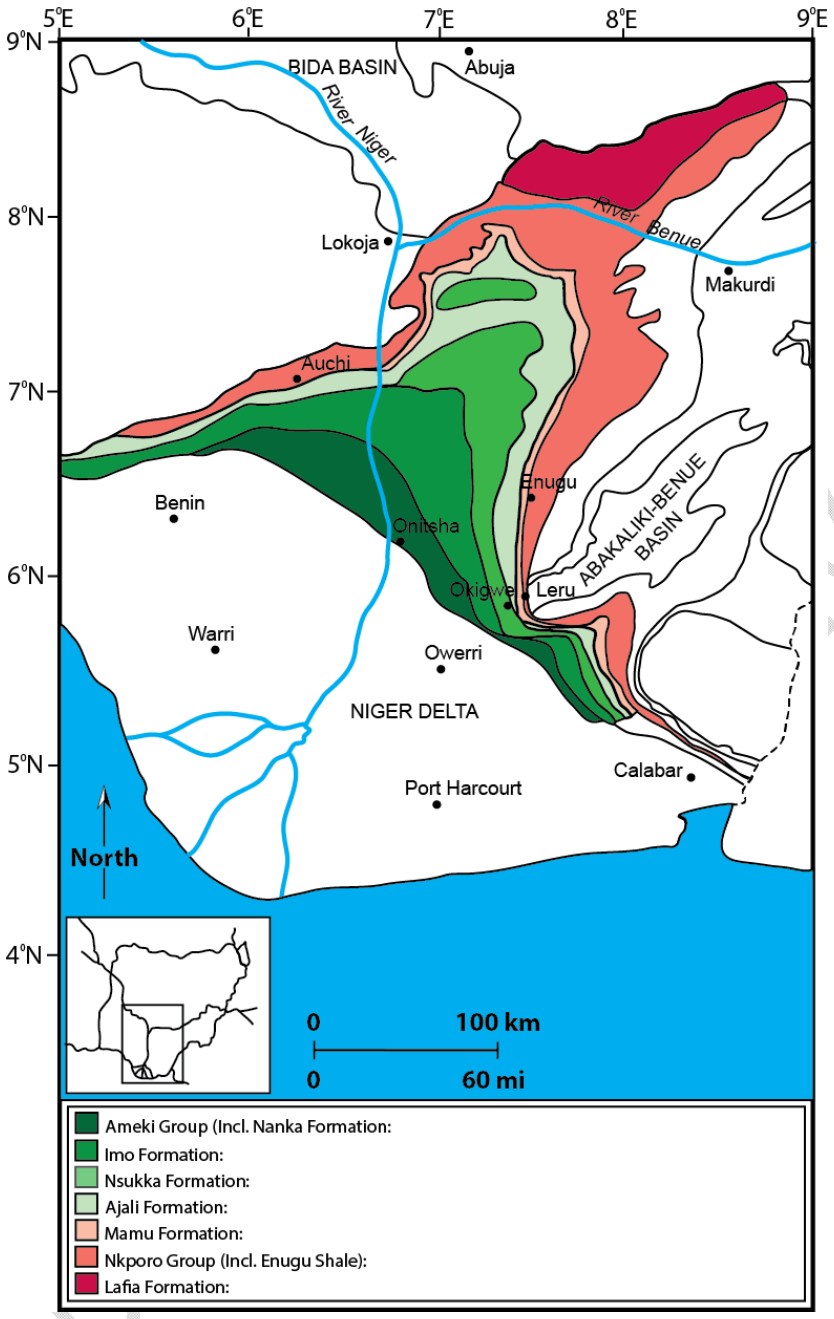

Figure 2. Geological map of Anambra Basin [20].

later became the primary depocentres for accumulation of sediment during the Campanian to Paleocene [24, 25, 26].

Sediments were sourced into the basin primarily from the Abakaliki Anticlinorium. Other sources of sediment input into the basin are crystalline basement areas of the Oban Massif and Cameroon basement to the right, and southwestern Nigeria craton to the left. The transgression that led to sediment deposition in the Campanian was short-lived and then, regression followed with more sediments accumulating to form the Campanian succession. The succession comprises Nkporo Shale, Owelli Sandstone and Enugu Shale, and together, they constitute the Nkporo Group. The Lokoja-Bassange Sandstone is the lateral equivalent of the Owelli Sandstone. These successions are succeeded by Mamu Formation, which comprises deltaic foresets and floodplain sediments. This formation is overlain by the continental sandstones of Ajali Formation, followed by Nsukka Formation [27, 28, 29, 30], which completes the stratigraphy in the southern Benue Trough (Figure 3).

2.2 Sediment Facies and Sedimentary Logs

Field observations and measurements during outcrop study formed the basis for facies identification, description, and classification in this study. Lithology definition and sedimentary structures were used to classify these facies into facies associations. Sedimentary logs generated at four selected positions across the outcrop provided information about facies composition and vertical relationships. Careful examination of outcrop across lateral and vertical extents was carried out to assess variation in facies succession, thickness, and lateral extent, and to delineate geometry of principal units in the sandstone body. The geometry and dimension for these units served as the basis for constructing the conceptual sedimentological model that describes the alluvial architecture of the sandstone body.

3. RESULTS

3.1 Sediment Lithofacies

In the braidplain sandstone body studied, three main facies associations are recognized based on dominant lithology. These facies associations are: pebbly sandstone (FA1), sandstone (FA2), and mudstone (FA3). In addition to grain size, array of sedimentary structures in these facies associations enables further classification into *facies* (Table 1). Description of these facies is provided in the following sub-sections.

3.1.1 Pebbly Sandstone

In the braidplain sandstone body, pebbly sandstone facies association (FA1) makes up a total of 20.5% of the outcrop (Table 2). The facies association is composed of fine to medium-grained pebbles of quartz that are largely sub-angular to sub-rounded. Within this facies association, isolated pebbles of quartzite and porphyritic igneous rock are common. Pebbles can be up to 2 cm in diameter and have their long-axis oriented parallel to bedding. FA1 is very poorly sorted and forms fairly large beds that extend laterally up to 4 m with sharp and erosive basal contacts. Three facies of pebbly sandstone were recognized based on their internal architecture: (1) inversely graded pebbly sandstone, (2) normally graded pebbly sandstone, and (3) chaotic-bedded pebbly sandstone.

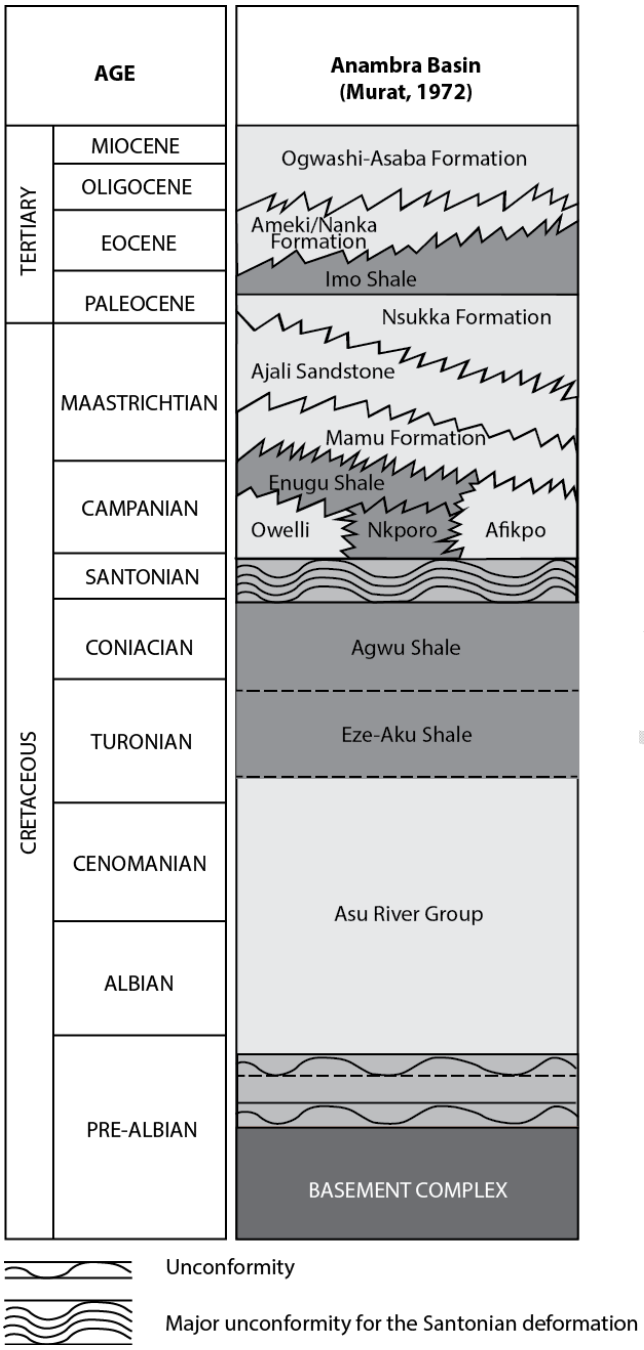

Figure 3. Generalized stratigraphic succession in the southern Benue Trough [reproduced from 25]. In the southern Benue Trough, the upliftment and folding of the Abakaliki Anticlinorium led to the exposure and subsequent erosion of the Coniacian, Turonian and Albian Formations.

Table 1. Classification of sediment lithofacies in the braidplain sandstone body at Ekpeshi.

Facies	Lithological characteristics	Sedimentary structures
FA1. Pebbly sandstone		
P1. Inversely graded pebbly sandstone	Mainly pebbles with <10% sand matrix, very poorly sorted, gradational contact	Inverse grading
P2. Normally graded pebbly sandstone	Poorly sorted at the base gradually fining upwards through granules to moderately sorted, medium grained sandstone	Normal grading, current ripples
P3. Chaotic-bedded pebbly sandstone	Very poorly sorted pebbly sandstone with irregular or disturbed beds of moderately sorted fine to medium-grained sandstone	Irregular bedding, disturbed lamination, stoss-side-missing current ripples
FA2. Sandstone		
S1. Structureless sandstone	Very poorly sorted, fine to coarse-grained sandstone with shards of claystone	Largely structureless except for discontinuous lenticular sands atop beds
S2. Tabular cross-bedded sandstone	Poorly sorted, coarse-grained sandstone with sparse fine quartz pebbles	Tabular cross bedding with planar foresets
S3. Flaser-bedded sandstone	Poorly sorted, coarse-grained sandstone with dispersed very fine pebbles	Discontinuous, non-parallel, flaser bedding with muddy silts in troughs
S4. Trough cross-bedded sandstone	Moderately sorted, medium-grained sandstone	Trough cross bedding
S5. Parallel horizontal-laminated sandstone	Poorly sorted, coarse-grained sandstone with floating clasts of claystone	Parallel horizontal lamination
S6. Lenticular-bedded sandstone	Very poorly to poorly sorted, medium to coarse-grained sandstone	Discontinuous, sub-parallel lenticular bedding, fading ripples, micro-cross lamination with very fine sand to coarse silt troughs
S7. Ripple-laminated sandstone	Moderately sorted, medium-grained sandstone	Current ripples, climbing ripples
S8. Ripple cross-laminated sandstone	Poorly to moderately sorted, medium-grained sandstone	Current ripple cross lamination
FA3. Mudstone		
M1. Claystone clasts	Dispersed and isolated claystone clasts in a matrix of poorly sorted sandstone	Pseudonodules, shards of claystone clasts

Table 2. Proportion of sediment lithofacies based on measured vertical sections.

Facies Association	Facies	Proportion of facies (%)
FA1. Pebbly sandstone	P1. Inversely graded pebbly sandstone	10
	P2. Normally graded pebbly sandstone	8
	P3. Chaotic-bedded pebbly sandstone	2.5
FA2. Sandstone	S1. Structureless sandstone	5
	S2. Tabular cross-bedded sandstone	12
	S3. Flaser-bedded sandstone	3
	S4. Trough cross-bedded sandstone	18
	S5. Parallel horizontal-laminated sandstone	7
	S6. Lenticular-bedded sandstone	12
	S7. Ripple-laminated sandstone	14
	S8. Ripple cross-laminated sandstone	8
FA3. Mudstone	M1. Claystone clasts	0.5

3.1.1.1 Inversely graded pebbly sandstone (P1)

Inversely graded pebbly sandstone is primarily composed of minor sand matrix, usually <10%. This facies is very poorly sorted (Figure 4A). It is marked by sharp and erosive basal contacts with trough cross-bedded sandstone (S4), ripple-laminated sandstone (S7) and ripple cross-laminated sandstone (S8). P1 exhibits gradational contact with overlying beds, particularly tabular cross-bedded sandstone (S2). The long axes of the pebbles are oriented parallel to bedding. The facies makes up 10% of the outcrop. It has average thickness of 0.6 m and its lateral extent is between 1.2 m and 5.5 m.

3.1.1.2 Normally graded pebbly sandstone (P2)

This facies is characterized by an organized internal architecture that differentiates it from the inversely graded pebbly sandstone (P1). In the sandstone body, P2 has a relative abundance of 8%. The facies is poorly sorted at the base and gradually fines upwards to moderately sorted medium-grained sandstone. Pebble population decreases upwards into dominantly sandstone unit (Figure 4B), which tends to be abruptly scoured by P1, thus bounding sharply with the overlying unit. The upper part of P2 is marked by ripple laminations. The facies is characterized by variable dimensions, ranging from 0.6 m to 1.2 m in thickness and 1.7 m to 12.0 m in lateral extent.

3.1.1.3 Chaotic-bedded pebbly sandstone (P3)

Unlike other pebbly sandstones, chaotic-bedded pebbly sandstone facies lacks organized internal architecture as a result of irregularity of bedding (Figure 4C). This facies makes up 2.5% of the outcrop. It consists of admixture of very poorly sorted pebbly sandstone and moderately

A.

B.

C.

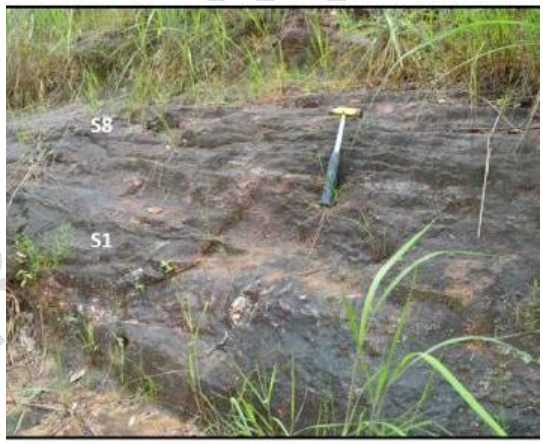

D.

D.

F.

G.

H.


I.


J.

Figure 4. Photographs of sediment facies in the braidplain sandstone body at Ekpeshi. The facies are classified based on dominant lithology, grain size, and sedimentary structures. (A) Inversely graded pebbly sandstone (B) Normally graded pebbly sandstone (C) Chaotic-bedded pebbly sandstone (D) Structureless sandstone and ripple cross-laminated sandstone (E) Tabular cross-bedded sandstone (F) Flaser-bedded sandstone (G) Trough cross-bedded sandstone; ripple-laminated sandstone (H) Parallel horizontal-laminated sandstone (I) Lenticular-bedded sandstone (J) Claystone clasts.

sorted fine to medium–grained sandstone. The chaotic internal structure comprises relics of beddings, laminations and current ripples. Clasts of siltstone and claystone are scattered throughout P3 intervals. Although its lateral extent exceeds 8.5 m, its thickness varies between 0.9 m and 1.2 m.

3.1.2 Sandstone

Sandstone facies association (FA2) makes up 79.0% of the braidplain sandstone body. This facies association comprises facies that are typically moderately sorted and devoid of pebbles barring dispersed clay clasts that are randomly distributed. Eight facies types are recognized in this facies association based on dominant internal structure. These facies are: structureless sandstone, tabular cross-bedded sandstone, flaser-bedded sandstone, trough cross-bedded sandstone, parallel horizontal-laminated sandstone, lenticular-bedded sandstone, ripple-laminated sandstone, and ripple cross-laminated sandstone.

3.1.2.1 Structureless sandstone (S1)

Structureless sandstone lacks organized internal architecture and well-defined bedding with the exception of discontinuous lenticular sands that cap individual beds (Figure 4D). These sand lenses occasionally display fading ripples. The relative abundance of this facies in the sandstone body is 5%. The facies comprises very poorly sorted fine to coarse-grained sandstone with shards of siltstone and claystone clasts that may be up to 3 cm in diameter. Both basal and top contacts are gradational. S1 beds are laterally extensive and range in thickness from 0.6 m to 2.0 m.

3.1.2.2 Tabular cross-bedded sandstone (S2)

In the sandstone body, the relative abundance of tabular cross-bedded sandstone is 12%. The facies comprises poorly sorted very coarse-grained sandstone with rare sub-rounded fine quartz pebbles. It bounds sharply with underlying P1 beds and overlying S3 beds. It has organized internal architecture that is characterized by tabular cross bedding with planar foresets (Figure 4E). S2 beds are laterally extensive without internal scours. Thickness of these beds, however, varies from 0.5 m to 1.0 m.

3.1.2.3 Flaser-bedded sandstone (S3)

Wavy laminated sandstone facies comprises poorly sorted coarse-grained sandstone. The facies makes up 3% of the outcrop; hence it is the least abundant sandstone facies in the sandstone body. Its internal architecture is dominated by flaser bedding with muddy silts in troughs (Figure 4F). S3 beds commonly make basal gradational contact with S2 beds. At the top, the facies bounds sharply with S5 or S7. S3 beds may be up to 15.0 m in lateral extent but rarely exceed 1.2 m in thickness.

3.1.2.4 Trough cross-bedded sandstone (S4)

Trough cross-bedded sandstone consists of moderately sorted medium-grained sandstone. The facies lacks internal grading and consists of sharp basal and top contacts with underlying S7 beds and overlying S6 beds. The relative abundance of this facies in the outcrop is 18%; hence it is the most abundant facies in the sandstone body. Internal structure in S4 intervals is primarily composed of trough cross bedding (Figure 4G).

Thickness of these intervals range from 0.9 m to 3.5 m. Due to a lack of planar bedding, lateral extent of these intervals cannot be measured.

3.1.2.5 Parallel horizontal-laminated sandstone (S5)

Parallel horizontal-laminated sandstone makes up 7% of the outcrop. The facies is composed of coarse-grained sandstone that is largely poorly sorted. S5 beds consist of floating clasts of claystone of variable diameters. These isolated clasts have random orientation. Internal architecture consists of horizontal lamination (Figure 4H). The facies is characterized by sharp basal contact, commonly bounding P1, and gradational top contact with S1, S3, and S7. Its beds are 0.9 m to 3.5 m thick and are over 12.0 m in lateral extent.

3.1.2.6 Lenticular-bedded sandstone (S6)

Lenticular-bedded sandstone has a relative abundance of 12% in the outcrop. The facies has a maximum thickness of 3.0 m and lateral extent ranging from 4.5 m to 12.0 m. It is composed of very poorly to poorly sorted, medium to coarse-grained sandstone. Sorting tends to be better in beds comprising fine sand. Bed contacts are gradational. Internal architecture in S6 beds is characterized by discontinuous, sub-parallel lenticular bedding, fading ripples, and micro-cross lamination with very fine sand to coarse silt troughs (Figure 4I). Normal grading from coarse sand to fine sand is prevalent in lenticular-bedded sandstone.

3.1.2.7 Ripple-laminated sandstone (S7)

In the outcrop, ripple-laminated sandstone facies comprises moderately sorted medium-grained sandstone. The facies lacks internal grading. Its internal architecture consists of well-preserved current ripples and, less commonly, climbing ripples (see Figure 4G). S7 beds may amalgamate to form over 2.0 m-thick bed. The facies is characterized by sharp or gradational basal and top contacts. It makes up 14% of the sandstone body.

3.1.2.8 Ripple cross-laminated sandstone (S8)

Ripple cross-laminated sandstone is composed of poorly to moderately sorted medium-grained sandstone (see Figure 4D). The facies is characterized by gradational basal contact with other facies e.g. structureless sandstone. Current ripple cross lamination distinguishes this facies from S7. Claystone clasts are conspicuously absent in S8 beds. The facies is laterally extensive and has a maximum thickness of 0.85 m. Relative abundance of S8 in the sandstone body is 8%.

3.1.3 Mudstone

The sandstone body lacks distinct mudstone intervals but comprises claystone clasts (M1), which makes up <1% of the outcrop. The facies is non-fissile and consists of claystone clasts that are up to 0.64 m in diameter (Figure 4J). It is common in P1 and P3 beds where they accumulate as rip-up clasts on scoured surface. Smaller clasts are observed to be randomly distributed across S1 and S5 beds.

3.2 Geometry and Dimension

The braidplain sandstone body of the Lokoja-Bassange Formation is characterized by channel morphology (Figure 5). The morphology is delineated by steep margins with thalwegs that are marked by a change in grain-size and thin veneer of pebbles on erosive surface, forming basal lags. This morphology is classified into three based on decreasing magnitude (Figure 6): (i) cross-bedded, tabular morphology with sheet geometry that extends laterally to maximum length of 1200 m and maximum thickness of 15 m, (ii) multistorey channel morphology with laterally stacked geometry that extends up to 90 m in length and 8 m in thickness, and (iii) single channel morphology with lenticular geometry, extending over lateral and vertical distances of 2-5 m and 1.7 m, respectively. As observed in the outcrop, the sandstone units are connected vertically, and thus, display vertical stack pattern. Amalgamation of beds developed laterally extensive channel-fill sequence, which terminates at the margins of another channel-fill sequence.

In the sandstone body, channel-fill sequence consists of pebbly sandstone and medium to very coarse sandstone. The pebbles have variable diameters in pebbly sandstone facies. Sandstone facies commonly succeed pebbly sandstone and vary in grain size, bed thickness and internal architecture. They form laterally extensive beds. However, these beds thin out towards channel margins. The lenticular-shaped scours vary in height from 0.15 m to 0.45 m and in length from 0.23 m to 1.80 m.

4. Discussion

4.1 Depositional Attributes

The braidplain sandstone body in this study is composed of three distinct sandstone units (see Figure 5) that are separated over much of the outcrop by fine-grained bedload sediments. Each of the units represents a period of channel activity that terminated with a river channel cutting down into it and depositing bedload sediments to form a new sandstone unit. The facies composition of the units, based on four sedimentary logs (Figure 7) at selected points across the sandstone body, is presented in Figure 8. However, the base of Unit 1 and the top of Unit 3 were not fully captured by these logs because they are partially exposed. Thus, there is a sampling bias towards the facies that typify the onset and peak of channel activity in Unit 1 and the waning and abandonment phase in Unit 3. The sampling bias also affects the thickness of these units.

4.1.1 Unit 1 Sandstone

Unit 1 sandstone represents the oldest unit in the braidplain sandstone body. This unit is composed of pebbly sandstone to coarse-grained sandstone with a wide range of sedimentary structures including inverse grading (P1), normal grading (P2), chaotic bedding (P3), flaser bedding (S3), trough cross bedding (S4), parallel horizontal lamination (S5), and ripple lamination (S7). Across the same bedding plane, Unit 1 sandstone is also found to be structureless (S1) and in certain places, comprises clay-rich rip-up clasts (M1). Based on comparison with Unit 2 sandstone, thickness of Unit 1 sandstone may exceed 5.0 m. However, only about 2.0 m of the thickness is exposed. The unit is composed of laterally connected sandstone that extends over a lateral distance of 750 m. Based on the log data, 32% of the sandstone unit is composed of trough cross-bedded

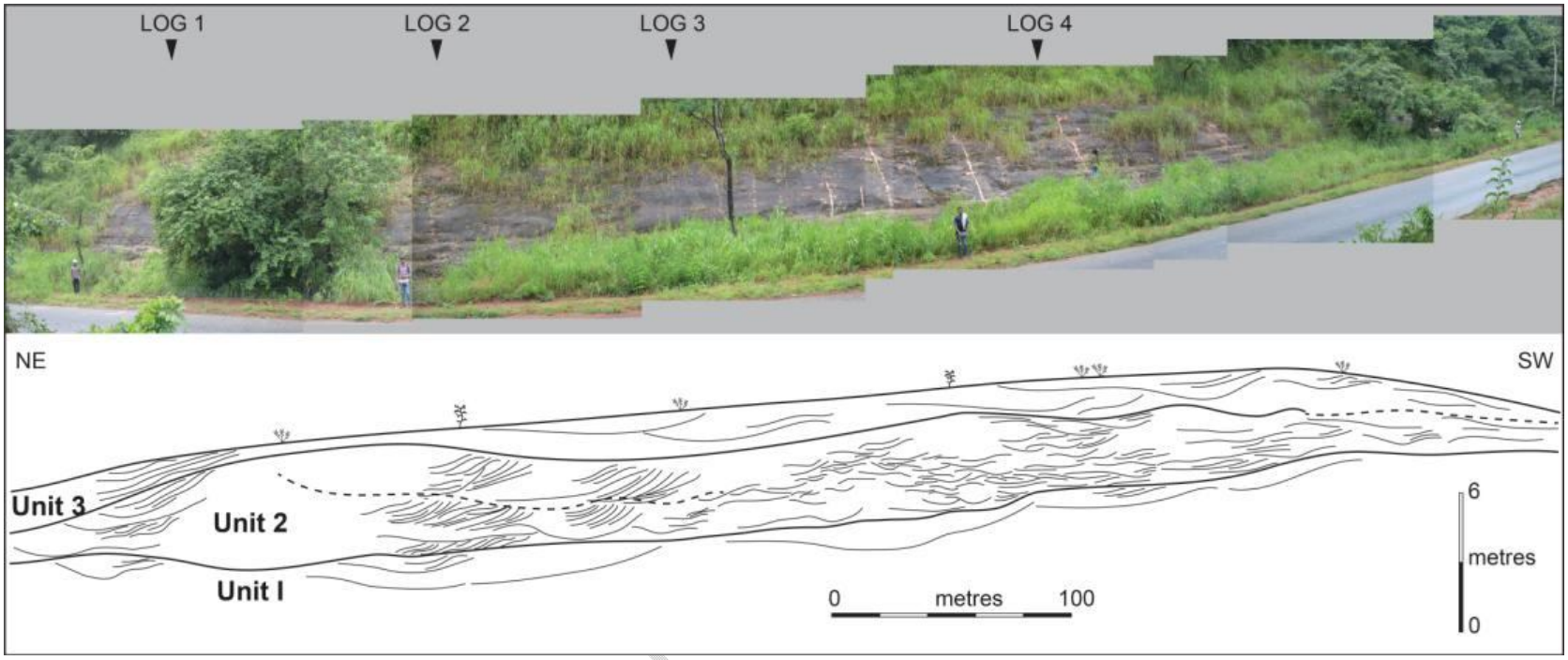

Figure 5. Morphology and geometry of the braidplain sandstone body at Ekpeshi. The sandstone body is characterized by sheet channel morphology with stepped geometry. Location of Logs 1-4 are indicated in the photograph.

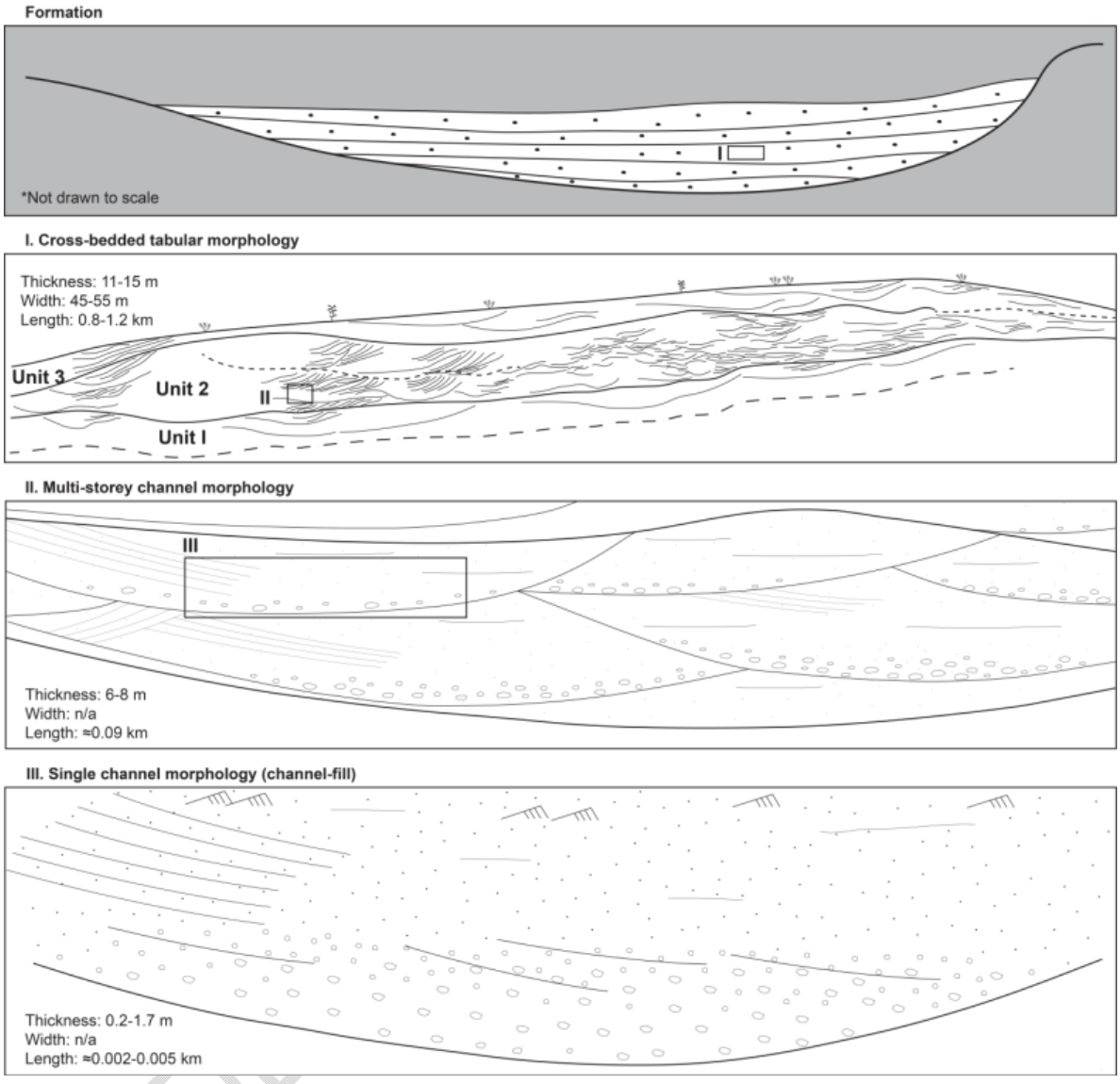

Figure 6. Hierarchy of sandstone units in the braidplain sandstone body at Ekpeshi.

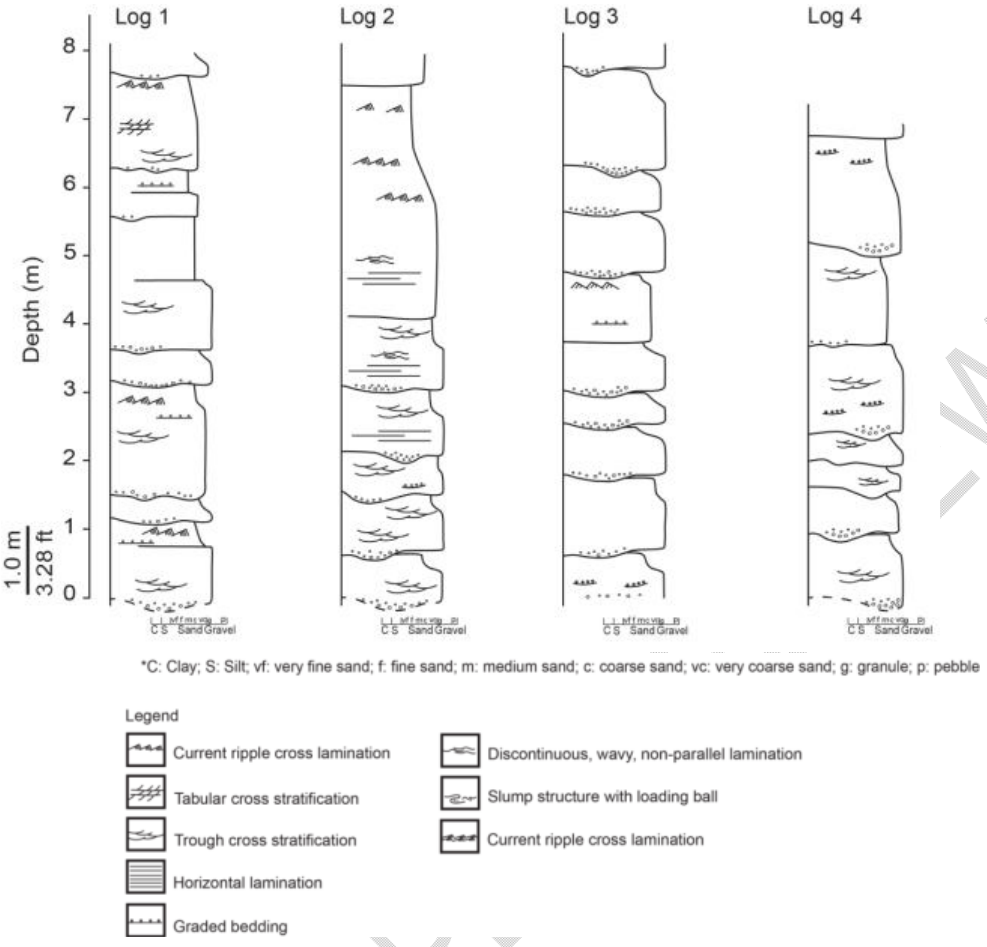

Figure 7. Sedimentary logs produced at selected points across the braidplain sandstone body. The logs show dominant sedimentary structures, variation in bed thickness and grain size. Base and top of the sandstone units are not exposed.

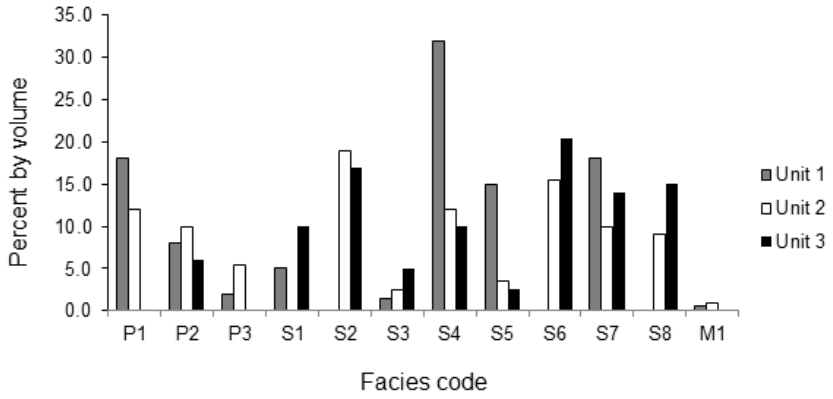

Figure 8. Comparative facies composition of Unit 1, Unit 2, and Unit 3 sandstones in the braidplain sandstone body.

sandstone (S4), followed by inversely graded pebbly sandstone (P1) and ripple-laminated sandstone (S7) with 18% apiece. Parallel horizontal-laminated sandstone (S5) and normally graded pebbly sandstone (P2) make up 15% and 8% of the unit, respectively. Five percent of the unit is composed of structureless sandstone (S1), whereas chaotic-bedded pebbly sandstone (P3), flaser-bedded sandstone (S3) and claystone clasts (M1) account for <5%.

4.1.2 Unit 2 Sandstone

Unit 2 sandstone is the intermediate unit between Unit 1 sandstone below and Unit 3 sandstone above. The unit, around 5.5 m thick, is the most laterally extensive of all the three sandstone units. It comprises sandstone of diverse grain sizes from pebbly to medium and a wide spectrum of sedimentary structures, which include inverse grading (P1), normal grading (P2), chaotic bedding (P3), tabular cross bedding (S2), flaser bedding (S3), trough cross bedding (S4), parallel horizontal lamination (S5), lenticular bedding/lamination (S6), ripple lamination (S7), and ripple cross-lamination (S8). Shards of claystone clasts (M1) are also common in Unit 2 sandstone, particularly in chaotic-bedded sandstone. The unit is characterized by vertical stack pattern. From the log data, 19% of the unit is composed of tabular cross-bedded sandstone (S2), whereas lenticular-bedded sandstone (S6) constitutes 15.5% of the unit. Both inversely graded pebbly sandstone (P1) and trough cross-bedded sandstone (S4) make up 12% each. By contrast, percent volume of normally graded pebbly sandstone (P2), ripple-laminated sandstone (S7), and ripple cross-laminated sandstone (S8) are 10%, 10% and 9%, respectively. Chaotic-bedded sandstone (P3), flaser-bedded sandstone (S3), and parallel horizontal-laminated sandstone (S5) have a combined percent volume of 11.5%. Dispersed claystone clasts (M1) is the least constituent facies by percent volume (<1%) in this sandstone unit.

4.1.3 Unit 3 Sandstone

Unit 3 sandstone is the youngest sandstone unit in the braidplain sandstone body. The unit has average thickness of 4.5 m, and comprises medium to very coarse sand with typical sedimentary structures that reflect organized internal structure such as normal grading (P2), tabular cross bedding (S2), flaser bedding (S3), trough cross bedding (S4), parallel horizontal lamination (S5), lenticular bedding (S6), ripple lamination (S7) and ripple cross lamination (S8). The unit lacks claystone clasts that are present in Units 1 and 2. The lateral continuity of channel sandstones in Unit 3 is marked by variable thickness across its lateral extent. Based on the log data, the unit is composed of 21% of lenticular-bedded sandstone (S6), 16% of tabular cross-bedded sandstone (S2), 15% of ripple cross-laminated sandstone (S8), and 14% of ripple-laminated sandstone (S7). Other facies constituents in this unit are structureless sandstone (S1) and trough cross-bedded sandstone (S4) that make up 10% apiece, and normally graded pebbly sandstone (P2), flaser-bedded sandstone (S3) and parallel horizontal-laminated sandstone (S5) that make up 6%, 5%, and 3%, respectively.

4.2 Alluvial Architecture

The architecture of the braidplain sandstone body is characterized by undulatory topography that developed from lateral bars in low-sinuosity braided river channel (Figure 9). During the activity phase of this SSW-NNE trending channel, pebbly sandstone was deposited first, followed by finer grained sediments. The river channel cut down about 5 m deep through mud-rich floodplain to deposit its channel sandstone. Migration of flow around these lateral bars led to laterally connected channel sandstone with multistorey stack pattern. The

succession in this unit suggests a complex history of bar migration during peak channel activity, and later, during waning stages of channel flow. The upward transition of in-channel pebbly sandstone facies to dominantly finer-grained sandstone facies reflects a sudden change in channel activity attributed to progressively reducing flow size and sediment load causing a vertical change in facies composition from normally graded pebbly sandstone (P2) to trough cross-bedded sandstone (S4), parallel horizontal-laminated sandstone (S5) and ripple-laminated sandstone (S8). This channel-fill sequence suggests that the abrupt transition may have been shorter in terms of lateral extent as a result of a river channel that was collapsing in size. Subsequent flows became larger in size and caused the river channel to expand. Increased sediment load during this period resulted in deposition of laterally continuous channel sandstone of Unit 2. The unit comprises channel sandstone with tabular cross bedding that is characterized by planar and curved foresets and trough cross bedding that downlap onto the top of Unit 1 sandstone. Water escaped structures that formed during high flow regime may have developed chaotic bedding in the channel-fill sequence. The dispersed claystone clasts (M1) in this unit can be attributed to broken pieces of claystone that fell into the river channel from channel banks at the peak of flow. The high flow regime associated with Unit 2 sandstone was followed by a period of reduced flow size with smaller sediment load causing abrupt upward transition from Unit 2 sandstone to Unit 3 sandstone with marked variable thickness across the channel width. The mudstone blanket that develops abandonment topography on the sandstone body marks the end of channel activity, and thus, represents abandonment facies that caps the channel-fill complex in the braidplain sandstone body.

4.3 Implications for Reservoir Development

The braidplain sandstone body of the Cretaceous Lokoja-Bassange Formation, exposed at Ekpeshi, is characterized by high net-to-gross ratio (95%) and excellent lateral continuity of channel sandstone units that develop multistorey and multilateral stack patterns. These architectural styles of channel sandstone will facilitate effective communication between reservoir layers during hydrocarbon production [31]. At distant view, the sandstone body is typified by sheet geometry with laterally extensive channel sandstone in a depositional system marked by clastic wedge geometry. Typical depositional systems with this geometry require a trapping mechanism for hydrocarbon to accumulate and impermeable floodplain mud to preserve it. The Peco oilfield of Alberta where a 20 m-deep and 3 km-wide braided channel complex is enclosed in impermeable floodplain deposits [32, 33] is a classic example. Lack of organized stratification and discontinuous shales in braidplain reservoirs may turn them into a single hydraulic unit with effective lateral displacement of fluids to production wells.

Channels in sand-rich low-sinuosity systems are characterized by downstream-accretion deposits that develop as lateral, longitudinal and transverse bars [34]. These deposits form in response to periods of active tectonism, rapid subsidence, and a large volume of sediment influx with thickness of 1 m to 1,200 m, width of 50 m to 1,300 km, and width-to-thickness ratio of 15 to 15,000 [35]. They comprise poor to moderately-sorted sand with variable proportion of pebbles and/or conglomerate, silt and dispersive clay. They form reservoirs that are known for excellent quality and high recovery factors. The minor interbedded shales in braidplain successions allow channel-fill sequences to develop multistorey and multilateral stack patterns that make them very productive reservoirs.

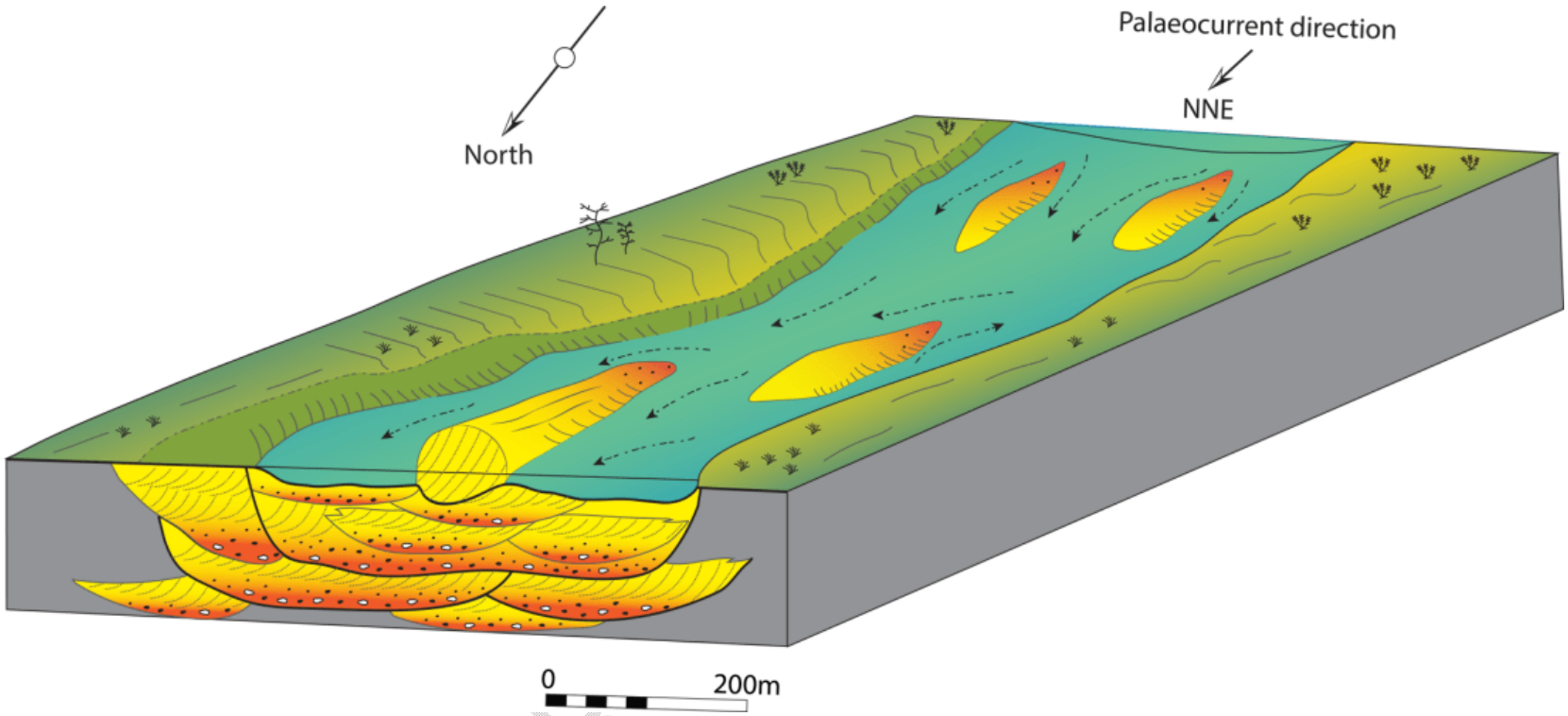

Figure 9. Conceptual sedimentological model of the braidplain sandstone body at Ekpeshi. The model captures geometrical framework of the sandstone body and reflects its alluvial architecture.

In braidplain reservoir successions, however, constituent sandbodies with similar textural attributes and composition may have dissimilar internal structure. Consequent upon the contrasting attributes, braidplain successions are typified by upward-decreasing permeability trends [36]. Because mud is not preserved in these successions, good vertical pressure communication has become commonplace in many reservoirs that are formed in braidplain settings. Although local shale barriers in these reservoirs may inhibit gas coning and water influx to wells [35], extensive floodplain mud that accumulate atop of bars in braidplain successions may act as barriers to flow. Cases in point include Jackson oil field in Australia [37], Budare oil field in Venezuela [38], and more. Lastly, randomly distributed shards of mudstone and diagenetically modified clay-rich rip-up clasts in these successions may form baffles to flow. A case in point is the Lower Cretaceous Cutbank Sandstone of Southern Alberta [39].

5. CONCLUSIONS

This outcrop-based study demonstrates the use of sedimentary attributes in analysis of sediment facies in a braidplain sandstone body in the Cretaceous Lokoja-Bassange Formation. As revealed in this study, the braidplain sandstone body is characterized by amalgamation of beds that resulted in multistorey and multilaterally-stacked channel sandstone units. In reservoirs with similar architecture, these stack patterns will facilitate effective pressure communication across producing reservoir intervals. Lack of organized stratification and discontinuous shales in these reservoirs may turn them into a single hydraulic unit with effective lateral displacement of fluids to production wells. On the flip side, the sheet geometry that typifies braidplain sandstone bodies requires a trapping mechanism for hydrocarbon to accumulate and impermeable floodplain mud to preserve it. Laterally extensive floodplain mud in these sandstone bodies, however, poses a major risk to vertical flow because of its potential for flow segregation across net pay intervals.

REFERENCES

1. Gibling MR. Width and thickness of fluvial channel bodies and valley fills in the geological record: a literature compilation and classification. Sedimentary Research. 2006; 76:731-770.
2. Martin JH. A review of braided fluvial hydrocarbon reservoirs: the petroleum engineer's perspective. In: Best JL, Bristow CS, editors. Braided Reservoirs. Special Publication No. 75. London: Geological Society. 1993; 333-367.
3. Bridge JS. Characterization of fluvial hyrocarbon reservoirs and aquifers: problems and solutions. Asociación Argentina de Sedimentología. 2001; 8(2):87-114.
4. Miall AD. The geology of fluvial deposits: sedimentary facies, basin analysis, and petroleum geology. Berlin: Springer; 2006.
5. Omoniyi BA. Fluvial facies and their reservoir potential: a concise review. International Journal of Scientific Research and Engineering Development. 2021; 4(4):1255-1266.
6. Melvin J, Knight AS. Lithofacies, diagenesis and porosity of the Ivishak Formation, Prudhoe Bay Area, Alaska. In: McDonald DA, Surdam RC, editors. Clastic Diagenesis. Memoir No. 37. Tulsa: American Association of Petroleum Geologists. 1984; 347-365.

7. Wicks JL, Buckingham ML, Dupree JH. Endicott Field: U.S.A. North Slope Basin, Alaska. Treatise V: Structural Traps. Tulsa: American Association of Petroleum Geologists. 1991; 1-25.
8. Hallett D. Petroleum Geology of Libya. Amsterdam: Elsevier BV; 2002.
9. Clifford HJ, Grund R, Musrati H. Geology of a stratigraphic giant: Messla oil field, Libya. In: Halbouty MT, editor. Giant Oil and Gas Fields of the Decade 1968-1978. Memoir No. 30. Tulsa: American Association of Petroleum Geologists. 1980; 507-524.
10. Lavering LH, Passmore VL, Paton IM. Discovery and exploitation of new oilfields in the Cooper-Eromanga Basins. Australian Petroleum Production & Exploration Association. 1986; 26(1):250-260.
11. Wiltshire MJ. Mesozoic stratigraphy and palaeogeography, eastern Australia. In: Proceedings of the Cooper and Eromanga Basins Conference. Petroleum Exploration Society of Australia, Society of Petroleum Engineers, Australian Society of Exploration Geophysicsists. 1989; 279-291.
12. Ghignone JI, De Andrade G. General geology and major oil fields in Recôncavo Basin, Brazil. In: Halbouty MT, editor. Geology of Giant Petroleum Fields: A Symposium. Memoir No. 14. Tulsa: American Association of Petroleum Geologists. 1970; 337-358.
13. Magnavita L, Da Silva RR, Sanches CP. Field trip guide of the Recôncavo Basin, NE Brazil. Boletim de Geosciencias. 2005; 13(2):301-333.
14. Inglis I, Gerard J. The Alwyn North Field, Blocks 3/9a, 3/4a, UK North Sea. In: Abbotts IL, editor. United Kingdom Oil and Gas Fields: 25 Years Commemorative Volume. Memoir No. 14. London: Geological Society. 1991; 21-32.
15. Gibbons KA, Jourdan CA, Hesthammer J. The Statfjord Field, Blocks 33/9, 33/12 Norwegian sector, Blocks 211/24, 211/25 UK sector, Northern North Sea. In: Gluyas JG, Hichens HM, editors. United Kingdom Oil and Gas Fields, Commemorative Millennium Volume. Memoir No. 20. London: Geological Society. 2003; 335-353.
16. Ellis AC, Kerr HM, Cornwell CP, Williams DO. A tectono-stratigraphic framework for Yemen and its implications for hydrocarbon potential. Petroleum Geoscience. 1996; 2:29-42.
17. Maycock I, Galbiati L (abstract). Alif Field: a giant field discovery in the Marib-Al Jawf Basin, Republic of Yemen. In: Proceedings of American Association of Petroleum Geologists Annual Meeting. Colorado, 3-6 June, 2001.
18. Bridge JS. Rivers and floodplains: forms, processes, and sedimentary record. Oxford: Blackwell Science Ltd; 2003.
19. Binks RM, Fairhead JD. A plate tectonic setting for Mesozoic rifts of West and Central Africa. Tectonophysics. 1992; 213:141-151.
20. Hoque M, Nwajide CS. Tectono-sedimentological evolution of an elongate intracratonic basin (aulacogen): The case of the Benue Trough of Nigeria. Mining and Geology. 1985; 21:19-26.
21. King LC. Outline and disruption of Gondwanaland. Geological Magazine. 1950; 87:353-359.
22. Benkhelil J. The origin and evolution of the Cretaceous Benue Trough (Nigeria). African Earth Sciences. 1989; 8:251-282.
23. Obi GC, Okogbue CO. Sedimentary response to tectonism in the Campanian-Maastrichtian succession, Anambra Basin, Southeastern Nigeria. Africa Earth Sciences. 2004; 38:99-108.
24. Burke KC, Dessauvagie TFJ, Whiteman AJ. Geological history of the Benue valley and adjacent areas. In: Dessauvagie TFJ, Whiteman AJ, editors. African Geology. Ibadan: University of Ibadan Press. 1972; 187-218.
25. Murat RC. Stratigraphy and paleogeography of the Cretaceous and Lower Tertiary in southern Nigeria. In: Dessauvagie TFJ, Whiteman AJ, editors. African Geology. Ibadan: University of Ibadan Press. 1972; 251-266.

26. Oboh-Ikuenobe FE, Obi CG, Jaramillo CA. Lithofacies, palynofacies, and sequence stratigraphy of Palaeogene strata in Southeastern Nigeria. Africa Earth Sciences. 2005; 41:79-101.
27. Akaegbobi IM, Boboye AO. Textural, structural features and microfossil assemblage relationships as a delineating criteria for the stratigraphic boundary between Mamu Formation and Nkporo Shale within the Anambra Basin, Nigeria. Nigerian Association of Petroleum Explorationist Bulletin. 1999; 14:176-193.
28. Hoque M, Ezepue MC. Petrology and paleography of the Ajali Sandstone. Sedimentary Petrology. 1977; 46:579-594.
29. Nwajide CS, Reijers TJA. Sequence architecture in outcrops: examples from the Anambra Basin, Nigeria. Nigerian Association of Petroleum Explorationist Bulletin. 1996; 11:23–33.
30. Onyekuru SO, Iwuagwu CJ. Depositional environments and sequence stratigraphic interpretation of the Campano-Maastrichtian Nkporo Shale Group and Mamu Formation exposed at Leru-Okigwe axis, Anambra Basin, Southeastern Nigeria. Australian Journal of Basic Applied Sciences. 2010; 4(12):6623-6640.
31. Dalrymple M. Fluvial reservoir architecture in the Statfjord Formation (northern North Sea) augmented by outcrop analogue statistics. Petroleum Geoscience. 2001; 7:115-122.
32. Gardiner S, Thomas DV, Bowering ED, McMinn LS. A braided fluvial reservoir, Peco field, Alberta, Canada. In: Barwis JH, McPherson JG, Studlick RJ, editors. Sandstone petroleum reservoirs. Berlin: Springer. 1990; 31-56.
33. Putnam PE. Fluvial deposits and hydrocarbon accumulations: examples from the Lloydminster area, Canada. In: Collinson JD, Lewin, J, editors. Modern and Ancient Fluvial Systems. Special Publication No. 6. Oxford: The International Association of Sedimentologists. 1983; 517-532.
34. Galloway WE, Hobday DK. Terrigenous Clastic Depositional Systems. New York: Springer-Verlag; 1983.
35. Shepherd M. Oil Field Production Geology. Tulsa: American Association of Petroleum Geologists; 2009.
36. Davies DK, Williams BPJ, Vessell RK. Dimensions and quality of reservoirs originating in low and high sinuosity channel systems, Lower Cretaceous Travis Peak Formation, East Texas, USA. In: North CP, Prosser DJ, editors. Characterization of Fluvial and Aeolian Reservoirs. Special Publication No. 73. London: Geological Society. 1993; 95-121.
37. Hunt JW, Guthrie DA, Dodman AP. Jackson field Australia Cooper-Eromanga Basins Central Australia. Treatise IV: Tectonic and Nontectonic Fold Traps. Tulsa: American Association of Petroleum Geologists. 1990; 217-253.
38. Hamilton DS, Tyler N, Tyler R, Raeuchle SK, Holtz MH, Yeh J, et al. Reactivation of mature oil fields through advanced reservoir characterization: a case history of the Budare field, Venezuela. American Association of Petroleum Geologists Bulletin. 2002; 86(7):1237-1262.
39. Farshori MZ (abstract). Fluvial facies and reservoir heterogeneity, Cutbank Sandstone (Lower Cretaceous), Horsefly Lake Pool, southern Alberta. In: Geology and Reservoir Heterogeneity. Canadian Society of Petroleum Geologists, Core Conference. 1989; 8.1-8.33.